Supporting information

Octopus-like flexible vector for noninvasive intraocular delivery of short interfering nucleic acids

Kuan Jiang[†], Yang Hu[†], Xin Gao[†] Changyou Zhan[†,‡], Yanyu Zhang[†], Shengyu Yao[†], Cao Xie[†], Gang Wei*[,†], Weiyue Lu[†]

[†]Key Laboratory of Smart Drug Delivery, Ministry of Education; Department of Pharmaceutics, School of Pharmacy, Fudan University, Shanghai 201203, China

[‡]Department of Pharmacology, School of Basic Medical Sciences, Fudan University, Shanghai 200032, China

Corresponding author:

Gang Wei, Ph.D., Professor

Key Laboratory of Smart Drug Delivery, Ministry of Education;

Department of Pharmaceutics, School of Pharmacy, Fudan University,

826 Zhangheng Road, Shanghai 201203, P.R.China

Tel: +86 21 51980091

Fax: +86 21 51980090

E-mail address: weigang@shmu.edu.cn

Methods

Cell Lines and Cultivation

Human corneal epithelial cells (HCEC, BNCC337876) and human conjunctival epithelial cells (NHC, ATCC CCL-20.2) were cultivated in DMEM (Gibco) supplemented with 10% FBS (Gibco) and 100 units/mL antibiotics (Penicillin-Streptomycin, Gibco) at 37°C in a 5% CO_2 humidified atmosphere. Human retinal pigment epithelial cells (ARPE-19, GNHu45) were cultivated in DMEM/F12 (Gibco) supplemented with 10% FBS and 100 units/mL antibiotics at 37°C in a 5% CO_2 humidified atmosphere. Human retinoblastoma cells (WERI-Rb-1, TCHu213) were cultivated in RPMI-1640 medium (Gibco) supplemented with 10% FBS and 100 units/mL antibiotics at 37°C in a 5% CO_2 humidified atmosphere. ARPE-19 and WERI-Rb-1 cells were kindly provided by Stem Cell Bank, Chinese Academy of Sciences.

Animals

Animals used in this work were obtained from the Experimental Animal Center of Fudan University and maintained at 22 ± 2°C on a 12 h light and dark cycle with access to food and water *ad libitum*. The animals for the experiments were treated according to protocols that were evaluated and approved by the Ethical Committee of Fudan University, and were acclimatized to laboratory conditions for 1 week prior to experiments. All animal procedures were performed in accordance with the ARVO Statement for the Use of Animals in Ophthalmic and Vision Research.

Synthesis and Characterization of Multivalent Penetratin

4-arm PEG-maleimide (1.0 mg, Mw 5.0 kD, Jenkem Technology) dissolved in 10 mM phosphate buffer (pH 7.2) mixed with Cys-capped penetratin (2.0 mg, ChinaPeptides) and stirred overnight under room temperature. Then the mixture was dialyzed (MWCO 7 kD) for 2 d in ice bath followed with a freeze drying process to obtain 4-valent penetratin (4VP). 8-valent penetratin (8VP) was prepared with a similar process. Molecular weight of 8-arm PEG-maleimide was 10 kD.

The purity and structure of multivalent penetratin were characterized via HPLC and ^{1}H NMR spectrum. Briefly, a Sepax Bio-C4 column (4.6 × 150 mm, 5 μm) was used at 25°C on a HPLC system (Agilent, United States). The mobile phase was acetonitrile (0.1% TFA): distilled water (0.1% TFA) at 5%-65% gradient in 30 min, at a flow rate of 0.8 mL/min, and UV absorbance of the effluent was monitored at 214 nm. The samples were dissolved in distilled water at a concentration of 5 mg/mL. ^{1}H NMR was performed on a 400 MHz NMR spectrometer (Varian, United States). The spectrum of samples dissolved in deuterium oxide at a concentration of 3.0 mg/mL was recorded at room temperature, and the scan times were 120.

Fabrication and Characterization of Polyplexes

Penetratin (Pe), 4VP and 8VP were mixed with ASO at different charge ratios (from 1:1 to 32:1, +/-) in Tris-EDTA buffer solution (pH=8.0), followed by a 30-s vortex and 30-min incubation at 37°C to form polyplexes Pe/ASO, 4VP/ASO and 8VP/ASO. These polyplexes were evaluated by a PAGE assay using 8% acrylamide and visualized under a chemiluminescent imaging system (Tanon 4200SF, China) after ASO was stained with GelRed (Biotium).

For the further formula screening, HCEC or NHC cells seeding on 12 well plates at a density of 2 × 10^4 cells/well were incubated with 8VP/ASO (ASO labeled with FAM) at different charge ratios for 1 h. After washed with 10 mM PBS for 3 times and trypsinized, cells were resuspended in 200 μL PBS and mean fluorescence intensity was measured by flow cytometer (BD, United States).

Based on the optimized formulation, ASO-contained and siRNA-contained polyplexes were separately prepared with same procedure. Besides, Lipofectamine™ 2000 (Invitrogen) was mixed

with nucleic acids at a ratio of 4:1 (vol_{Lipo} : $wt_{nucleic\ acids}$) to prepare Lipo/ASO according to the instruction (3.3-8.3 μL Lipofectamine per μg ASO or siRNA). Polyplexes morphology was observed under transmission electron microscope (FEI, United States) after drop-dried on a carbon copper grid. Particle size and zeta potential were tested by laser particle analyzer (Malvern, U.K.). Particle size variation with time at 34°C was also recorded. Fluorescence spectrum and intensity of FAM-labeled ASO or siRNA-contained polyplexes at different concentrations were measured by fluorescence spectrophotometer (Agilent, United States).

ASO (Sangon, China) sequence: 5'-CCUCUUACCUCAGUUACA-3', phosphorothioate modified. The siRNA (GenePharma, China) was designed to block the Fluc gene expression with the following sequence, antisense strand 5'-GCACUCUGAUUGACAAAUAdTdT-3', phosphorothioate modified, sense strand 5'-UAUUUGUCAAUCAGAGUGCdTdT-3', phosphorothioate modified.

Cytotoxicity and Cellular Uptake of Polyplexes

HCEC, NHC, ARPE-19 or WERI-Rb-1 cells at the logarithmic growth phase cultivated on 96 well plates at a primary cell density of 2×10^3 cells/well were incubated with the polyplexes at several concentration gradients. After 4 h, the former three cells were washed 3 times with 10 mM PBS, followed by further cultivation in 200 μL complete medium for 24 h, while WERI-Rb-1 cells were directly treated with CCK-8 reagent (Meilun Biotech, China) for 4 h at 37°C. The former three cells were incubated with 0.5 mg/mL MTT agent in each well for 4 h at 37°C, and produced formazan was dissolved in 150 μL DMSO. The OD_{490} was measured via microplate reader (Bio-Tek, United States).

For quantitative evaluation of cellular uptake of the polyplexes, HCEC, NHC, ARPE-19 or WERI-Rb-1 cells cultivated on 12 well plates at a primary density of 2×10^4 cells/well were incubated with different polyplexes for 4 h. After washed with 10 mM PBS containing 0.02 mg/mL heparin sodium for 3 times and trypsinized (unnecessary for WERI-Rb-1 cells), cells were resuspended in 200 μL 10 mM PBS and the amount of FAM-positive cells and mean fluorescent intensity were tested by flow cytometer (BD, United States).

NHC cells cultivated on 35mm 4-chamber glass bottom dishes (Cellvis, United States) at a primary density of 1×10^4 cells/well were incubated with ASO-contained polyplexes for 4 h. Then the medium was carefully sucked followed by a step of washing cells with 10 mM PBS containing 0.02 mg/mL heparin sodium. Finally, cells immersed in glycerine/10 mM PBS (1:1, volume ratio) were observed under confocal laser scanning microscope (Carl Zeiss, Germany).

Inhibition of Protein Expression in Fluc/GFP-positive Cells

Lentiviral vectors encoding firefly luciferase (Fluc) and green fluorescent protein (GFP) were used to infect WERI-Rb-1 cells to obtain co-expressed cells (Fluc/GFP-Rb-1). To identify the transfection efficiency, infected cells were observed under the inverted fluorescence microscope (Leica, Germany) and the GFP-positive cells were also counted by the flow cytometer. Meanwhile, transfected cells were seeded in the 24 well plates and bioluminescence intensity was detected under the IVIS Spectrum system (Cailper PerkinElemer, United States) 15 min after the D-luciferin potassium salt (0.15 mg/mL, Sciencelight) was added.

To evaluate inhibition effects of siRNA-contained polyplexes on Fluc protein expression in the Fluc/GFP-Rb-1 cells, the cells cultivated on the 24 well plates at a primary density of 5×10^4 cells/well were incubated with the polyplexes for 4 h in complete medium containing 10% FBS, with a further cultivation in fresh complete medium for 20 h. The bioluminescence intensity was

measured as mentioned above.

Transport Efficacy of Polyplexes across an *in vitro* BRB Model

The *in vitro* BRB model was established as previously reported with slight modification.[1, 2] Briefly, ARPE-19 and HUVEC cells were seeded on the front and contrary of rat tail collagen type I coated Corning 6.5 mm polyester membrane filters (pore size 0.4 μm) at the density of 1×10^4 cells/well. Transepithelial electrical resistance (TEER) was measured by an epithelial volt-Ωm (Millipore, USA) to estimate the barrier integrity. Barriers with TEER over 100 $\Omega \cdot cm^2$ were chosen for the transfer experiments. The apical side of barriers was incubated with the polyplexes in 100 μL D-Hank's balanced salt solution (D-HBSS, pH7.2) while the basolateral side was 600 μL D-HBSS. An aliquot of 400 μL of sample was extracted from the basolateral side every 0.5 h, and followed with supplement of 400 μL fresh D-HBSS. Fluorescence intensity of the original sample and the sample mixed with isovolumetric 2 M NaOH or 0.2 M phosphate buffer (PB, pH 7.4) was measured by microplate reader. Post-transported barriers were observed under confocal laser scanning microscope.

Intraocular Distribution and Pharmacokinetics Behavior of Polyplexes

Male mice (18 - 20 g) derived from Institute of Cancer Research, United States were used in this experiment. The polyplexes dissolved in 5 μL artificial tear fluid were instilled in the conjunctival sac of mice, and the total dose of FAM-labeled ASO was 2.64 μg/eye. The eyelids were gently pulled up and down to keep homodisperse on the ocular surface. After instillation, the mice were sacrificed (injection with the fatal dose of pentobarbital sodium, 150 mg/kg) 10 min, 30 min, 1 h, 2 h, 4 h, 6 h later and the eyeballs were gathered to fix in Davidson's solution for 30 min. Then the eyeballs were moved into 30% sucrose for overnight dehydration. DAPI-dyed frozen sections were observed under an inverted fluorescence microscope.

Inhibition of Luciferase Expression in an Intraocular Orthotopic Tumor Model

Intraocular orthotopic tumor-bearing mice were established as reported before.[3] Briefly, the male Balb/c nude mice were anesthetized by intraperitoneal injection with 40 mg/kg pentobarbital sodium in combination with topical application of 0.4% oxybuprocaine hydrochloride, followed by instillation of 0.5% tropicamide to dilate the pupil. Fluc/GFP-Rb-1 cells (2×10^4 cells suspended in 2 μL 10 mM PBS) were injected slowly into the vitreous cavity of the right eye using a microsyringe (33 G, Hamilton), followed by instillation of 0.5% levofloxacin. Ocular luminescence of the mice were detected in the following days and the tumor-bearing mice were randomly divided into four groups (n = 4). The mice were treated with 5 μL of 10 mM PBS, naked siRNA, Lipo/siRNA and 8VP/siRNA via topical instillation from day 0 (treatment beginning) to day 15 (3 times daily, equal to 1 μg siRNA daily). The mice were intraperitoneal injected with 150 mg/kg D-luciferin and anesthesia by isoflurane 15 min before luminescence signal was detected via the IVIS Spectrum system. *In vivo* imaging was carried out on day 0, 3, 5, 7, 9, 11, 13 and 15. After treatment, the mice were sacrificed (injection with the fatal dose of pentobarbital sodium, 150 mg/kg) and the treated eyes were fixed in 4% paraformaldehyde and dyed with hematoxylin-eosin (HE) for further observation under inverted fluorescence microscope.

Statistical analysis

Statistical significances of the quantitative data were analyzed by the One-way ANOVA multiple comparisons corrected by Dunnett test. It was considered that $p > 0.05$ was not significant (ns), $^*p < 0.05$ was significant, and $^{**}p < 0.01$ even $^{***}p < 0.001$ was highly significant.

Results

Considering the number of tentacles might play an important role in the *in vitro* and *in vivo* behaviors of MVPs, we designed and synthesized both 4VP and 8VP via a single-step addition reaction between the maleimide group at the end of each PEG arm and the thiol group at the N-terminus of cysteine (Cys) capped penetratin.[4] Both 4VP and 8VP were of high purity (> 95%) and yield (~100%) ascertained by HPLC and ^{1}H NMR spectra (Fig. S1).

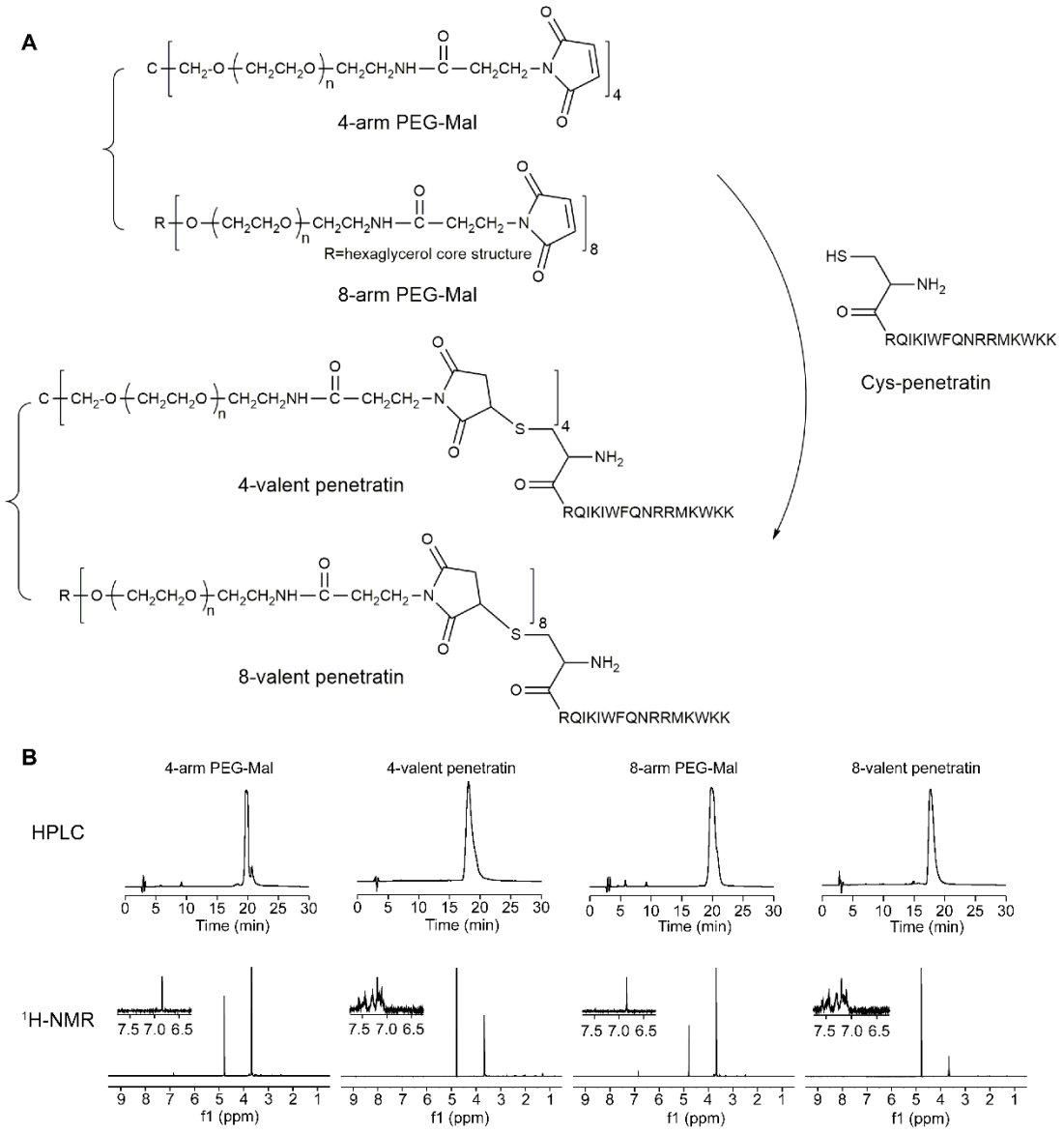

Figure S1 Synthesis and characterization of multivalent penetratin (MVP). A Sepax Bio-C4 column (4.6 × 150 mm, 5 μm) was used at 25°C for HPLC analysis. The mobile phase was acetonitrile (0.1% TFA): distilled water (0.1% TFA) at 5% to 65% gradient in 30 min, at a flow rate of 0.8 mL/min, and UV absorbance of the effluent was monitored at 214 nm. The ^{1}H NMR spectra of samples dissolved in deuterium oxide was recorded at room temperature, and the scan times were 120. The concentration of samples was 5.0 mg/mL for HPLC and 3.0 mg/mL for ^{1}H NMR.

To optimize the formation of polyplexes, polyacrylamide gel electrophoresis (PAGE) assay and quantitative cellular uptake were conducted. As shown in Fig. S2A, free ASO could be found in the electrophoresis image even at charge ratio between free penetratin and ASO (Pe/ASO) higher than

16:1 (+/-), suggesting free penetratin a poor condenser for ASO by itself. In contrast, 4VP and 8VP could efficiently condense ASO into stable polyplexes at the charge ratio higher than 8:1 (+/-). Furthermore, quantitative cellular uptake of 8VP/ASO at the charge ratio over 8:1 was investigated in both HCEC and NHC cells. When the charge ratio was 12:1, the cellular uptake showed an inflection point both in HCEC and NHC cells (Fig. S2B and S2C). Heavily cationic vectors always play a double-edged role, inducing high gene delivery efficiency while safety concerns.[5] Thus, 12:1 was chosen as the optimal charge ratio of polyplexes in the following experiments.

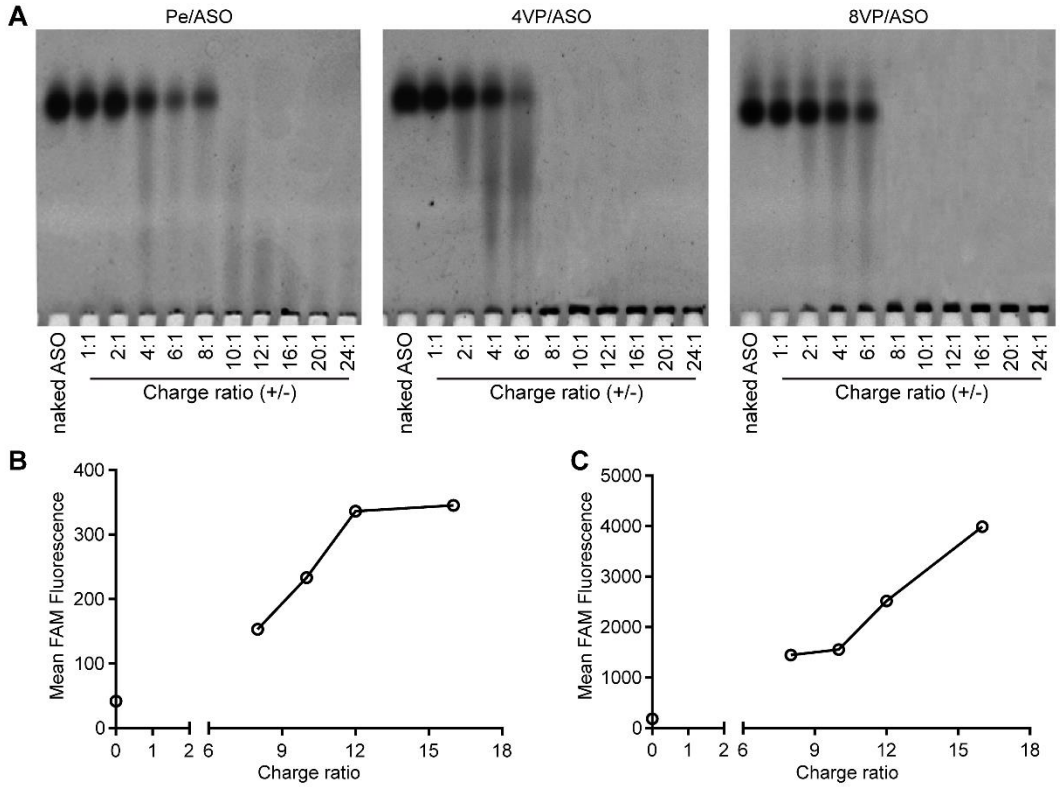

Figure S2 Prescription screening of polyplexes composed of MVP and antisense oligonucleotides (ASO). A, charge ratio (+/-) screening of the polyplexes by polyacrylamide gel electrophoresis. ASO was stained with GelRed and the images were recorded at 302 nm. B, C, quantitative cellular uptake of polyplex 8VP/ASO at different charge ratios in HCEC and NHC cells. All the polyplexes contained the same amount of FAM-labeled ASO (200 nM) and incubated with the cells for 1 h at 37°C.

Apart from fluorescence intensity, fluorescence spectra of the polyplexes also exhibited differences. The fluorescence intensity of Pe/ASO was too low to detect fluorescence emission spectrum (Fig. S3). Fluorescence spectra of 4VP/ASO were similar to naked ASO, but 8VP/ASO showed higher signal intensity in 600-800 nm range in excitation spectrum and lower intensity at the maximum emission wavelength, probably due to better shielding of FAM-labeled ASO by 8VP. Those results indicated that there was confirmed interaction between MVP and ASO.

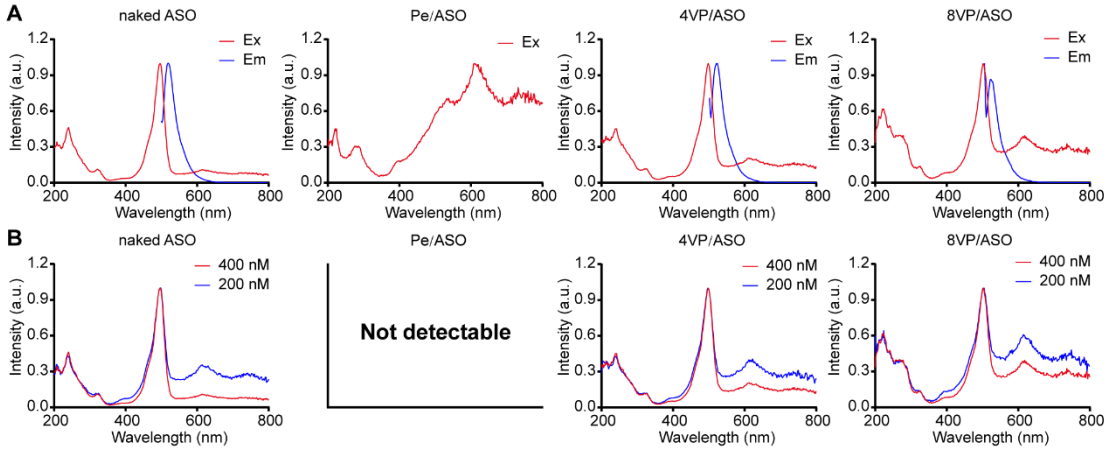

Figure S3 Fluorescence characteristics of ASO-contained polyplexes. A, fluorescence spectra of the polyplexes contained 400 nM FAM-labeled ASO. Ex, excitation spectrum, Em, emission spectrum. Emission spectra of naked ASO, 4VP/ASO and 8VP/ASO were determined at their own maximum excitation wavelength (496 nm, 498 nm, 502 nm, respectively). B, fluorescence excitation spectra of the polyplexes contained 200 nM or 400 nM ASO. Fluorescence spectra of Pe/ASO was not detectable. The polyplexes were dispersed in 10 mM PBS (pH 7.4).

In HCEC cells, mean fluorescence intensities of the cells treated by 4VP/ASO and 8VP/ASO were about 10 and 50 times higher than those treated by naked ASO (Fig. S4A). Besides, the proportions of single live cell among total events were 93.7%, 94.5% and 95.1% for the blank cells, 4VP/ASO and 8VP/ASO treated cells, respectively, but the number for Lipo/ASO treated cells was only 17.1% (Fig. S4B). Similar proportions of single live cell and cellular distributions meant MVP/ASO had slight effects on HCEC cells. In contrast, much lower proportion of single live cell after treated by Lipo/ASO revealed the potential cytotoxicity.

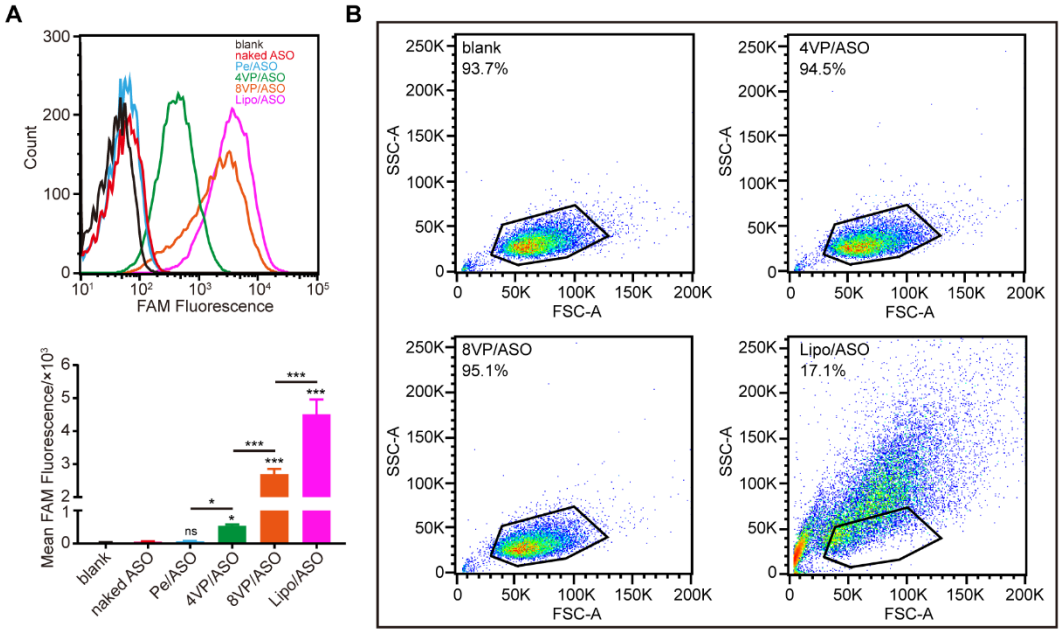

Figure S4 Cellular uptake of ASO in HCEC cells. A, flow cytometry profiles of the polyplexes and histogram of the mean fluorescence intensity in HCEC cells. B, pseudocolor scatter plots of forward scatter (FSC) and side scatter (SSC) for HCEC cells under testing condition. Values in each plot represent proportions of single live HCEC cell among total events. All polyplexes contained the same amount of FAM-labeled ASO (200 nM). The incubation lasted for 4 h at 37°C. The data are presented as mean ± standard deviation (SD) (n = 3, $^{ns}p > 0.05$, $^{*}p < 0.05$, $^{***}p < 0.001$, compared to naked ASO)

As shown in Fig. S5, for NHC cells treated with 4VP/ASO and 8VP/ASO, more FAM-labeled ASO (green) distributed in cytoplasm and most of them were not colocalized with lysosomes (red), indicating potential endosomal escape ability of MVP/ASO. However, for the cells treated by naked ASO or Pe/ASO, much less FAM-labeled ASO could be found in cytoplasm. Lipo/ASO treated cells did not tend to attach on the culture plates, causing difficulty in observation under microscope. In the same circumstance, more late endosomes or lysosomes were produced in the cells treated by Lipo/ASO than other polyplexes. Lipo/ASO was larger in particle size and rich in positive charge, therefore would induce lysosome rupture after being endocytosed, which might render cells susceptible to lysosomal death pathways.[6]

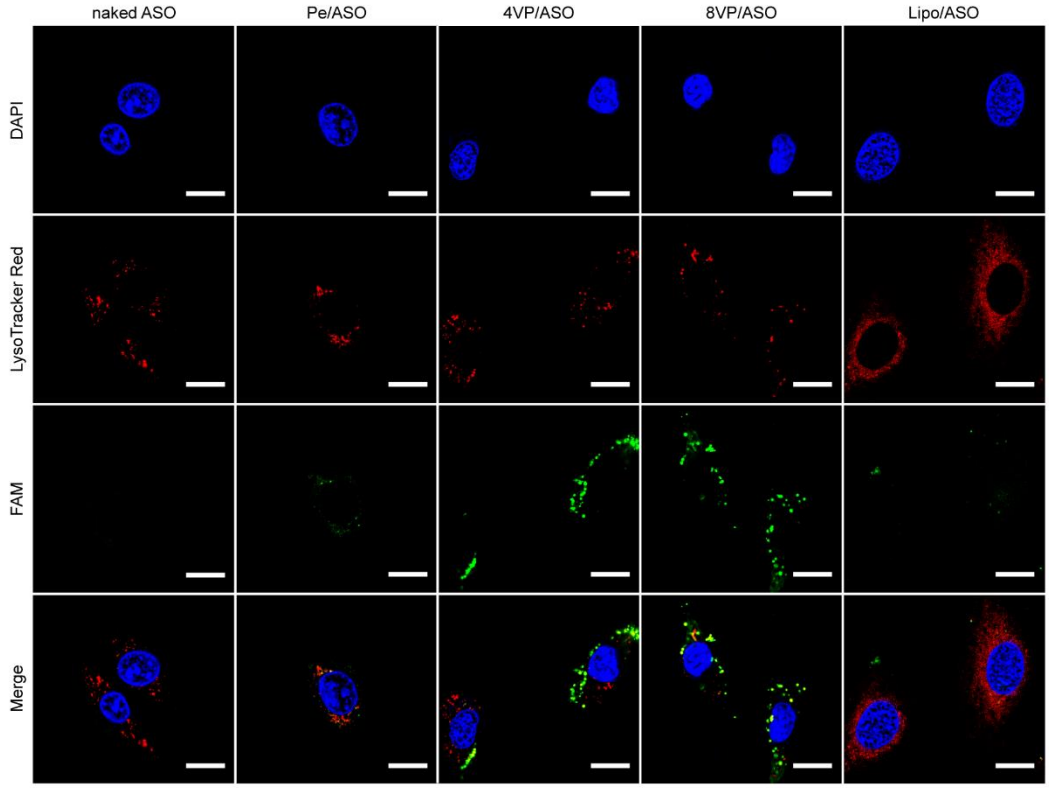

Figure S5 Intracellular distribution of polyplexes loading with FAM-labeled ASO (green). The nuclei of NHC cells were stained with DAPI (blue) while lysosomes were stained with LysoTracker Red DND-99 (red). Scale bar, 20 μm. All the formulations contained the same amount of FAM-labeled ASO (200 nM). The incubation lasted for 4 h at 37°C.

At a concentration up to 3.2 μM ASO, 16 times higher than the ceiling in cellular experiments, the viability of MVP/ASO treated cells was still more than 80% (Fig. S6), which indicated biosecurity

of MVP/ASO.

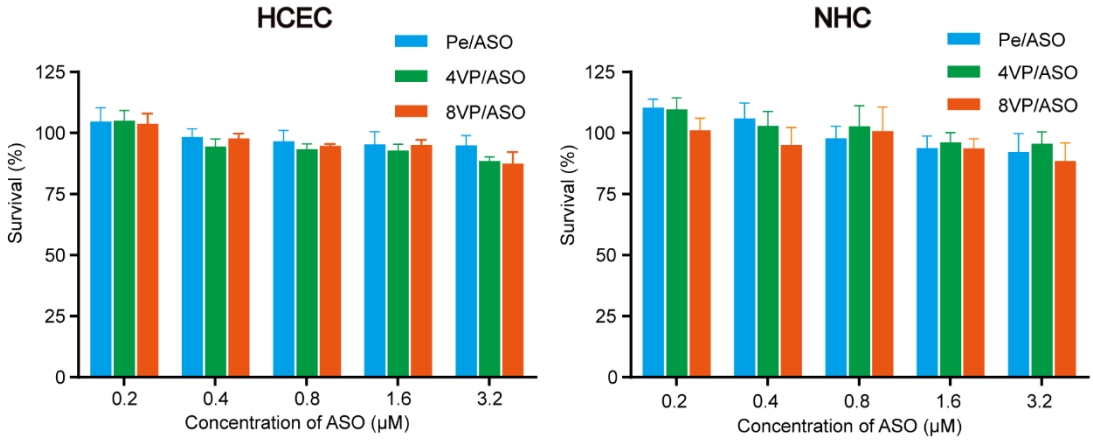

Figure S6 Cytotoxicity of polyplexes to HCEC and NHC cells. Cells were incubated with Pe/ASO, 4VP/ASO and 8VP/ASO at a series of concentrations for 12 h and a further cultivation in complete medium for 12 h. Results were expressed as the percentage compared to the untreated cells via a MTT assay. The data are presented as mean ± standard deviation (SD) (n = 5).

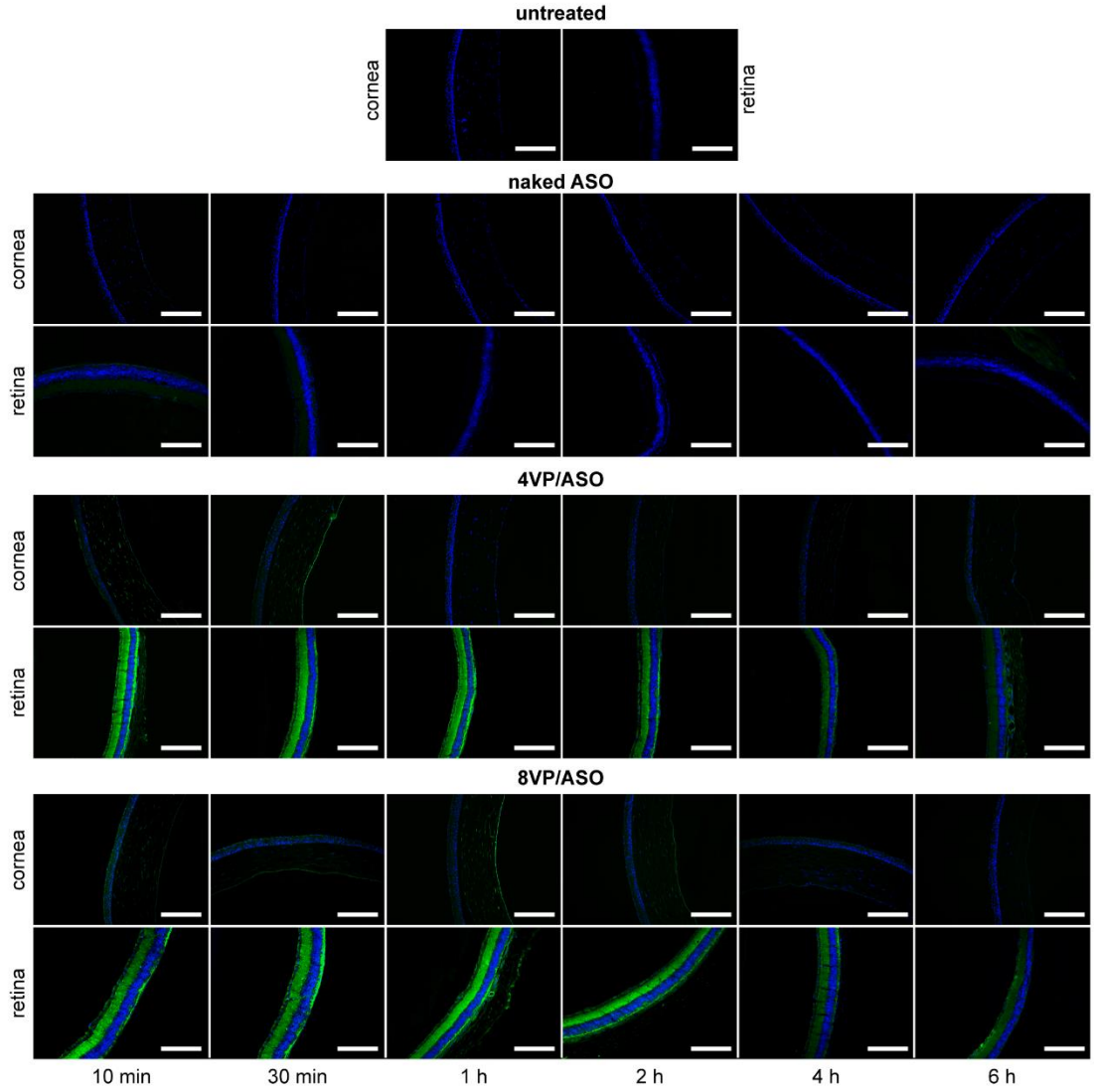

Figure S7 Time-dependent distribution of FAM-labeled ASO in DAPI-stained corneas and retinae from the mice treated by different polyplexes. The polyplexes containing same amount of ASO (2.64 μg/eye) in 5 μL artificial tear fluid were instilled into the conjunctiva sac of mice every 10 min for three times. Eyes were harvested at 10 min, 30 min, 1 h, 2 h, 4 h and 6 h after the last instillation. Scale bar, 100 μm.

Sections of the untreated eye did not emit any green fluorescence throughout the eye, revealing there was no fluorescence interference in the ocular tissues under the tested condition (Fig. S7). Topical instillation of naked ASO induced no perceptible green fluorescence in both anterior and posterior segments. For Pe/ASO treated eye, there was only weak green fluorescence in anterior and posterior segments. However, when treated by 4VP/ASO or 8VP/ASO, the eye emitted distinct green fluorescence, especially in the retina.

Particle size of Pe/siRNA was 515 nm, about 3 times larger than 4VP/siRNA (156 nm) and 6 times larger than 8VP/siRNA (85 nm), revealing that penetratin alone was incompetent to condense larger gene molecules, probably due to its dispersive positive charge (Table S1, Fig. S8A and S8B). Polydispersity index (PDI) of freshly prepared polyplexes was lower than 0.3, demonstrating their homogeneous size distribution. All the polyplexes exhibited a positive zeta potential, and more tentacles led to a relatively higher result. When using a commercial transfection reagent, Lipofectamine, to condense siRNA, particle size was about 420 nm, zeta potential higher than +40 mV, and notably PDI over 0.3. After incubation for 48 h, particle sizes increased about 30 nm for 4VP/siRNA and 15 nm for 8VP/siRNA (Fig. S8C). The polyplexes formed with siRNA were more stable than those with ASO, probably due to stronger electrostatic interaction between MVP and siRNA, which possesses denser electronegativity than ASO.[7]

Table S1 Particle size, polydispersity index and zeta potential of different polyplexes.

Abbreviation	Particle size (d. nm)	Polydispersity index	Zeta potential (mV)
Pe/ASO	152.7 ± 0.6	0.075 ± 0.019	+ 20.8 ± 0.9
4VP/ASO	139.9 ± 2.3	0.191 ± 0.013	+ 11.4 ± 1.0
8VP/ASO	95.1 ± 0.5	0.239 ± 0.019	+ 20.6 ± 1.1
Lipo/ASO	355.2 ± 16.2	0.301 ± 0.034	+ 20.2 ± 3.9
Pe/siRNA	514.8 ± 45.7	0.204 ± 0.201	+ 7.34 ± 0.8
4VP/siRNA	156.3 ± 2.7	0.115 ± 0.037	+ 12.1 ± 0.6
8VP/siRNA	85.4 ± 0.6	0.169 ± 0.014	+ 15.7 ± 0.4
Lipo/siRNA	419.6 ± 71.1	0.500 ± 0.375	+ 43.6 ± 1.0

The data are presented as mean ± standard deviation (SD) (n = 3).

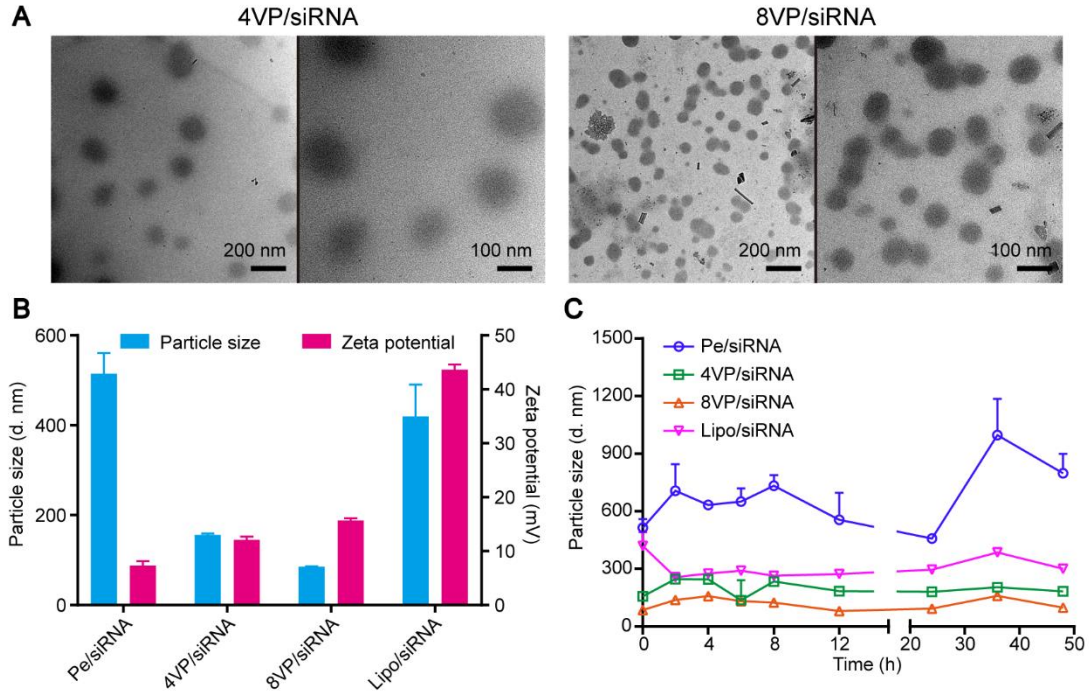

Figure S8 Characterization of siRNA-contained polyplexes. A, morphology of the polyplexes under the transmission electron microscope. B, particle sizes and zeta potentials of the polyplexes. C, time-dependent particle size variation of the polyplexes incubated in 10 mM PBS at 34 ± 0.5°C.

Differences in fluorescence characteristics of the polyplexes were obvious when free penetratin and MVP were separately used to condense siRNA. Compared to FAM-labeled naked siRNA, fluorescence intensity of the polyplexes containing same amount of nucleic acids decreased dramatically (Fig. S9A). In particular, the fluorescence of 8VP-based polyplexes decreased 4.2 times compared to naked siRNA at a concentration of 400 nM, while 2.8 times for 4VP-based polyplexes. Fluorescence intensity of MVP-based polyplexes decreased in a concentration-dependent manner (R^2>0.98) suggestive of high stability against dilution. In contrast, serial dilution of Pe/siRNA caused sharp change in fluorescence intensity (from 400 nM to 200 nM), indicating dissociation of free penetratin and nucleic acids from the polyplexes. Free penetratin with a dispersive charge distribution might have an "extensive" interaction with siRNA, resulting in different fluorescence spectra of Pe/siRNA compared to naked siRNA (Fig. S9B). Fluorescence spectra of 4VP/siRNA were basically same with naked siRNA, except higher signal intensity in 600-800 nm range in excitation spectrum, probably driven by interaction between 4VP and siRNA. Notably, 8VP/siRNA exhibited totally different fluorescence spectra compared to naked siRNA, which meant a distinctly different status of siRNA when binding with 8VP. The difference in excitation spectra of 8VP/siRNA and Pe/siRNA also reflected their differences in structure. Furthermore, double dilution did not change the fluorescence excitation spectrum of MVP-based polyplexes, but for Pe/siRNA, an emerging peak at about 490 nm revealed structure detriment of the polyplex after dilution, which was consistent with the results in fluorescence intensity variation (Fig. S9C).

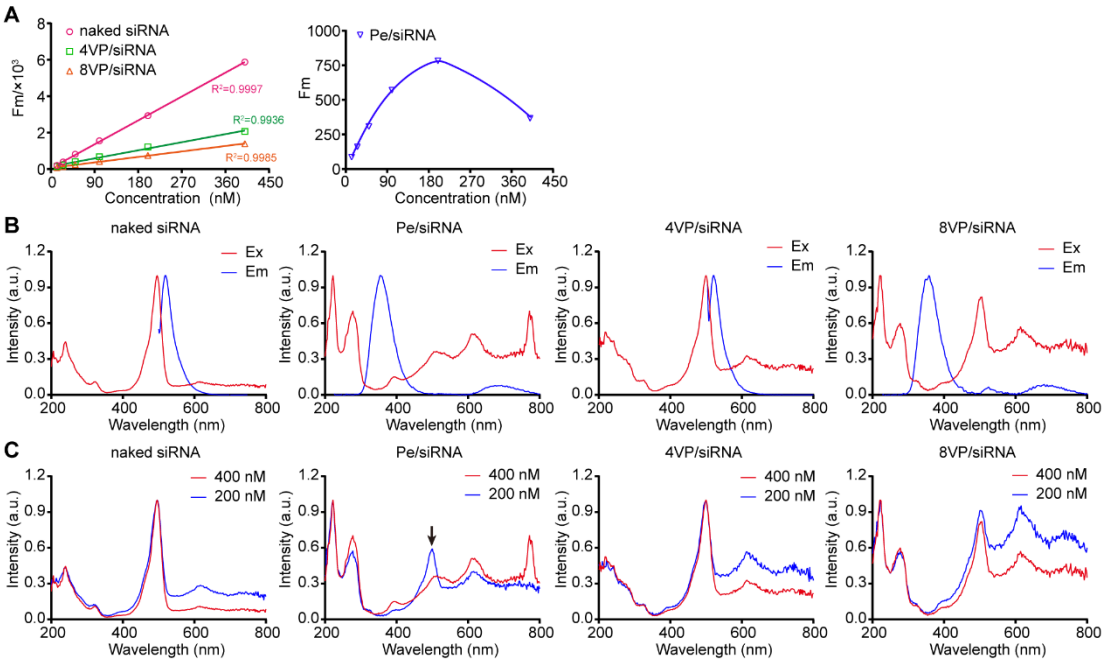

Figure S9 Fluorescence characteristics of siRNA-contained polyplexes. A, mean fluorescence intensity (Fm) of the polyplexes at different concentrations (FAM-labeled siRNA). Ex 490 nm, Em 520 nm. B, fluorescence spectra of the polyplexes at a concentration of 400 nM. Ex, excitation spectrum, Em, emission spectrum. Emission spectra of naked siRNA, Pe/siRNA, 4VP/siRNA and 8VP/siRNA were determined at their own maximum excitation wavelength (496 nm, 222 nm, 500 nm, 222 nm, respectively). C, fluorescence excitation spectra of the polyplexes at a concentration of 200 nM and 400 nM siRNA. The polyplexes were dispersed in 10 mM PBS (pH 7.4).

For cellular uptake of the polyplexes in human retinal pigment epithelial cells (ARPE-19), as shown in Fig. S10A and S10B, there was no statistically significant difference ($p > 0.05$) in mean fluorescence intensity between naked siRNA and Pe/siRNA treated cells, indicating that penetratin alone was inefficient to mediate intracellular delivery of siRNA into ARPE-19 cells. As for 4VP/siRNA and 8VP/siRNA, mean fluorescence intensity were 5 and 80 times higher than naked siRNA in ARPE-19 cells, respectively. Additionally, proportions of single live cell were similar for naked siRNA, 4VP/siRNA and 8VP/siRNA (82.5%, 76.0%, 73.6%) treated ARPE-19 cells, revealing MVP/siRNA was safe to ARPE-19 cells under tested concentration (Fig. S10C). For Lipo/siRNA treated cells, the proportion of single live cell sharply decreased to 3.11%, which revealed Lipo/siRNA had obvious cytotoxicity to ARPE-19 cells. Besides, it was also unable to obtain statistically significant quantitative data of cellular uptake from Lipo/siRNA treated ARPE-19 cells due to limited number of single live cell. When incubated with Pe/siRNA and MVP/siRNA at a concentration of lower than 318 nM siRNA for 4 h, the viability of ARPE-19 cells was over 80% (Fig. S10D). However, 50% inhibitive concentration (IC_{50}) of Lipo/siRNA on ARPE-19 cells was about 139 nM, which was lower than the concentration used in cellular uptake experiments (200 nM).

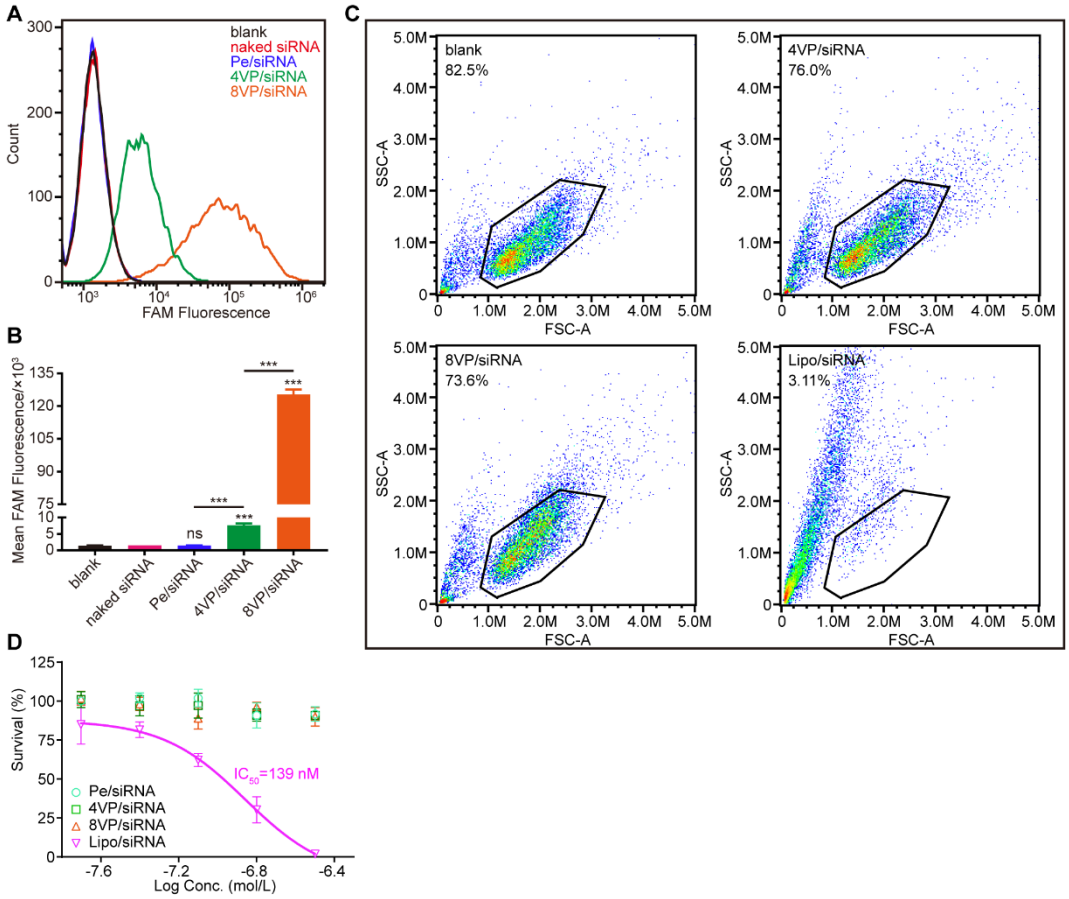

Figure S10 Quantitative cellular uptake and cytotoxicity of siRNA-contained polyplexes in ARPE-19 cells. A, B, flow cytometry profiles of the polyplexes and histogram of the mean fluorescence intensity were displayed. C, the populations of single live ARPE-19 cell were identified by FSC/SSC gating under testing condition. Values in each plot represent proportions of single live ARPE-19 cell among total events. All the polyplexes contained 200 nM FAM-labeled siRNA. D, cytotoxicity of the polyplexes to ARPE-19 cells. Results were expressed as percent of the values obtained from untreated cells. The incubation lasted for 4 h at 37°C. The data are presented as mean ± standard deviation (SD) (n = 3 for A and B, n = 5 for D, $^{ns}p > 0.05$, $^{***}p < 0.001$, compared with naked siRNA)

For cellular uptake of the polyplexes in human retinoblastoma cells (WERI-Rb-1), as shown in Fig. S11A and S11B, there was no statistically significant difference ($p > 0.05$) in mean fluorescence intensity between naked siRNA and Pe/siRNA treated cells, indicating that penetratin alone was inefficient to mediate intracellular delivery of siRNA into WERI-Rb-1 cells. As for 4VP/siRNA and 8VP/siRNA, mean fluorescence intensity were 3 and 7 times higher than naked siRNA in WERI-Rb-1 cells, respectively. For WERI-Rb-1 cells, proportions of single live cell were 43.3%, 39.8%, 38.9% and 0.58% for naked siRNA, 4VP/siRNA, 8VP/siRNA and Lipo/siRNA treated cells, respectively (Fig. S11C). Mean fluorescence intensity of Lipo/siRNA treated cells was not presented due to limited number of single live cell.

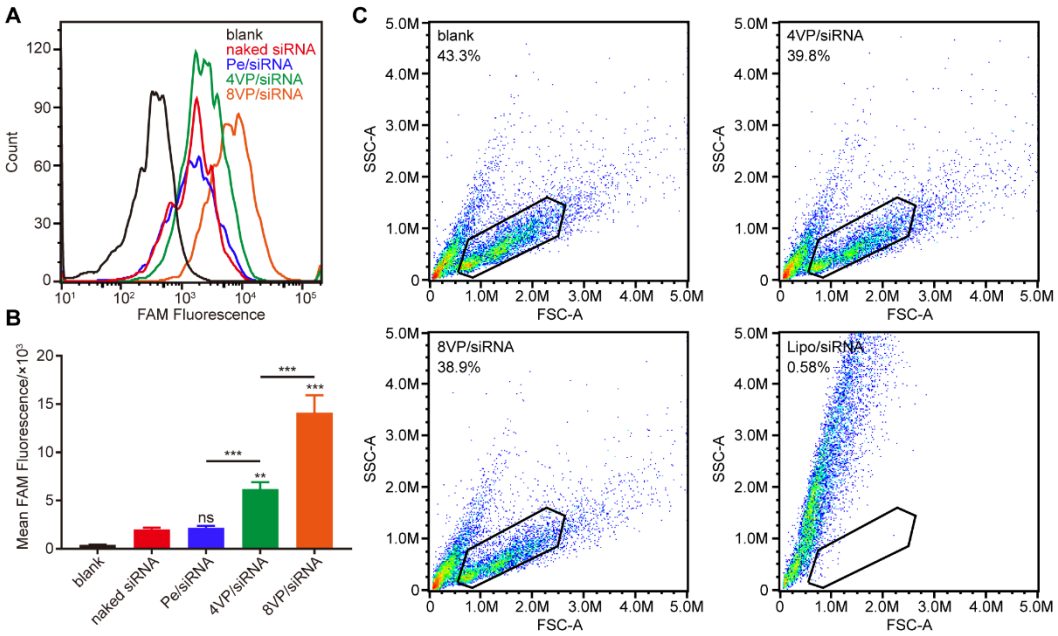

Figure S11 Quantitative cellular uptake of siRNA-contained polyplexes in WERI-Rb-1 cells. A, B, flow cytometry profiles of the polyplexes and histogram of the mean fluorescence intensity. C, the populations of single live WERI-Rb-1 cell were identified by FSC/SSC gating under testing condition. Values in each plot represent proportions of single live WERI-Rb-1 cell among total events. All the polyplexes contained 200 nM FAM-labeled siRNA. The incubation lasted for 4 h at 37°C. The data are presented as mean ± standard deviation (SD) (n = 3, $^{ns}p > 0.05$, $^{**}p < 0.01$, $^{***}p < 0.001$, compared to naked siRNA).

GFP expression was firstly evaluated to screen the dual-positive cells. According to the fluorescence images (Fig. S12A), most of cells emitted distinct green fluorescence, which was also proven by the quantitative measurement of GFP-positive cells. After immediately transfected (*Passage 0*), the percentage of GFP-positive cells was 92.7% (Fig. S12B), which was increased to 94.3% at *Passage 4* and 94.9% at *Passage 10*. Therefore, transfected cells at *Passage 4* to *Passage 10* were used for the further experiments. Intracellular Fluc expression was also evaluated. As shown in Fig. S12C, there was a good linear relationship (R^2=0.9907) between cell counts (ranging from 2×10^4 to 1×10^5) and bioluminescence intensity, indicating a uniform Fluc expression in Fluc/GFP-Rb-1 cells.

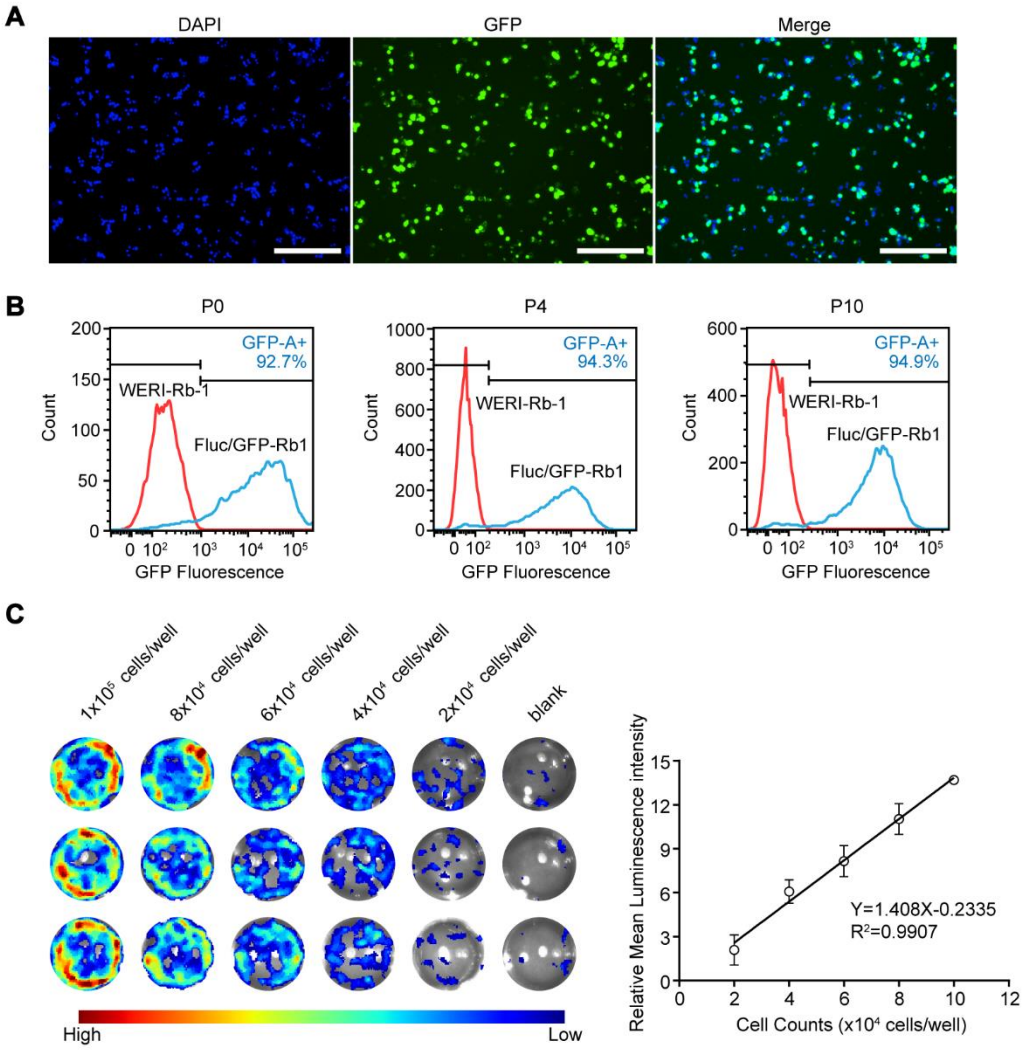

Figure S12 Characterization of protein expression in Fluc/GFP-Rb-1 cells. A, fluorescence images of cells with DAPI stained nucleus (blue). Scale bar, 200 μm. B, quantitative GFP expression in cells. The tested cells were at *Passage 0*, *4* and *10*, respectively. The WERI-Rb-1 cells were used as the blank control. C, bioluminescence intensity of cells at a series of densities. The data are presented as mean ± standard deviation (SD) (n = 3).

Ocular irritation of polyplexes was also evaluated. For the eyes exposed to 10 mM PBS, naked siRNA, 8VP/siRNA and Lipo/siRNA, there was no histological alteration in cornea after receiving TID treatment for 15 d (Fig. S13), indicating they were safe to the cornea under the therapeutic regimen.

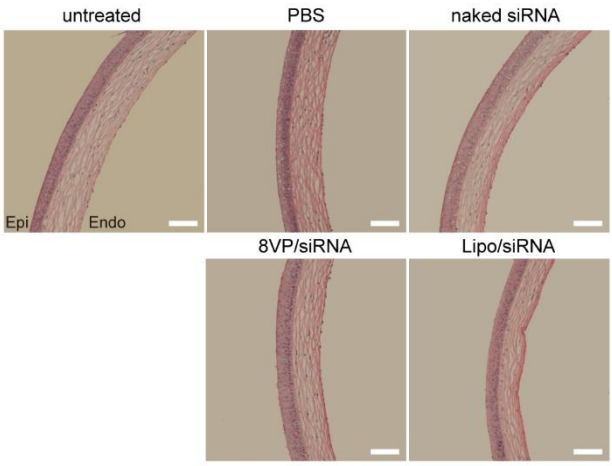

Figure S13 Hematoxylin-eosin stained paraffin sections of treated cornea from tumor-bearing mice after treatment for 15 d. Scale bar, 100 μm. Epi, epithelium, Endo, endothelium.

Reference

1. Hornof, M.; Toropainen, E.; Urtti, A. *Eur. J. Pharm. Biopharm.* **2005**, 60, 207-225.
2. Hamilton, R. D.; Leach, L. *Methods Mol. Biol.* **2011**, 686, 401.
3. Lemaitre, S.; Poyer, F.; Marco, S.; Freneaux, P.; Doz, F.; Aerts, I.; Desjardins, L.; Cassoux, N.; Thomas, C. D. *Invest. Ophthalmol. Visual Sci.* **2017**, 58, 3055-3064.
4. Martínez-Jothar, L.; Doulkeridou, S.; Schiffelers, R. M.; Sastre Torano, J.; Oliveira, S.; van Nostrum, C. F.; Hennink, W. E. *J. Controlled Release* **2018**, 282, 101-109.
5. Bloquel, C.; Bourges, J. L.; Touchard, E.; Berdugo, M.; BenEzra, D.; Behar-Cohen, F. *Adv. Drug Delivery Rev.* **2006**, 58, 1224-1242.
6. Kirkegaard, T.; Jäättelä, M. *Biochim. Biophys. Acta, Mol. Cell Res.* **2009**, 1793, 746-754.
7. Chi, X.; Gatti, P.; Papoian, T. *Drug Discovery Today* **2017**, 22, 823-833.